Smart Structures and Systems, Vol. 9, No. 5 (2012) 393-410
DOI: http://dx.doi.org/10.12989/sss.2012.9.5.393

An optical fibre monitoring system for evaluating the performance of a soil nailed slope

Hong-Hu Zhu*[1], Albert N.L. Ho[2], Jian-Hua Yin[3], H.W. Sun[4], Hua-Fu Pei[3] and Cheng-Yu Hong[3]

[1]*School of Earth Sciences and Engineering, Nanjing University, Nanjing 210093, China*
[2]*Ove Arup & Partners Hong Kong Limited, Hong Kong, China*
[3]*Department of Civil and Structural Engineering, The Hong Kong Polytechnic University, Hung Hom, Kowloon, Hong Kong, China*
[4]*Geotechnical Engineering Office, Civil Engineering and Development Department, Government of the Hong Kong Special Administrative Region, Hong Kong, China*

(Received October 11, 2010, Revised March 1, 2012, Accepted March 3, 2012)

Abstract. Conventional geotechnical instrumentation techniques available for monitoring of slopes, especially soil-nailed slopes have limitations such as electromagnetic interference, low accuracy, poor longterm reliability and difficulty in mounting a series of strain sensors on a soil nail bar with a small-diameter. This paper presents a slope monitoring system based on fibre Bragg grating (*FBG*) sensing technology. This monitoring system is designed to perform long-term monitoring of slope movements, strains along soil nails, and other slope reinforcement elements. All these *FBG* sensors are fabricated and calibrated in laboratory and a trial of this monitoring system has been successfully conducted on a roadside slope in Hong Kong. As part of the slope stability improvement works, soil nails and a toe support soldier-pile wall were constructed. During the slope works, more than 100 *FBG* sensors were installed on a soil nail, a soldier pile, and an in- place inclinometer. The paper presents the layout and arrangement of the instruments as well as the installation procedures adopted. Monitoring data have been collected since March 2008. This trial has demonstrated the great potential of the optical fibre monitoring system for long-term monitoring of slope performance. The advantages of the slope monitoring system and experience gained in the field implementation are also discussed in the paper.

Keywords: optical fibre sensing; soil nailing; slope monitoring system; fibre Bragg grating (*FBG*); geotechnical instrumentation

1. Introduction

Long-term stability of slopes involves interactions of various environmental factors (e.g., water ingress through surface infiltration and runoff, subsurface groundwater flow and external loading) and ground conditions (e.g., geological and weathering profiles as well as hydrogeological conditions). In Hong Kong's hilly terrain, there are thousands of natural and man-made slopes and slope failure sometimes occurs, especially in the rain seasons. The geotechnical profession in Hong Kong has made a lot of efforts on slope safety. Given the dense population and its high vulnerability to landslides, there is a need for the profession to devote continued efforts to further understand performance of slopes,

*Corresponding author, Associate Professor, E-mail: zhh@nju.edu.cn

especially slopes affected by adverse geological and hydrogeological conditions. Regarding the movements and stability condition of a slope, there are still a number of issues not fully understood. For example, rainfall infiltration has been recognized as an important factor affecting the stability of unsaturated soil slopes (Fredlund and Rahardjo 1993, Gasmo *et al.* 1999, Ng *et al.* 2003, Li *et al.* 2005, Zhang *et al.* 2006). However, few researchers have conducted studies on the effects of rainfall and the corresponding groundwater responses on structural components which are used to stabilize the slopes.

To improve our understanding of performance of slopes in adverse environmental conditions, slope monitoring is one of the most effective approaches, which would reduce uncertainties in design assumptions and provide useful data for post-construction performance review (Wong *et al.* 2006, Millis *et al.* 2008). Manufacturers of geotechnical instruments have developed different types of products for slope engineering (Dunnicliff 1993). However, these existing techniques for slope monitoring have certain limitations, including electromagnetic interference (*EMI*), low accuracy, poor long-term durability, and various installation difficulties. In the past few decades, new technologies such as Global Positioning System (*GPS*) and Time Domain Reflectometer (*TDR*) are being developed for use in slope movement measurement (Ding *et al.* 2003, Yin *et al.* 2004, Lin and Tang 2005, Peyret *et al.* 2008). However, their accuracy still cannot meet the requirement of geotechnical engineers.

In recent years, optical fibre sensors have been developed rapidly for structural health monitoring (*SHM*) of important or sensitive infrastructures (e.g., bridges and dams). In comparison with conventional transducers as well as some of recently developed field instrumentation techniques, optical fibre sensors have apparent advantages, such as immunity to electromagnetic interference, better resistance to corrosion, high precision and tiny size. fibre Bragg gratings (*FBG*), lowcoherence interferometry (*LCI*), optical time domain reflectometry (*OTDR*) and Fabry-Perot interferometry (*FPI*) and nonlinear techniques such as Raman and Brillouin scattering, are among the various types of optical fibre sensing technologies available (Inaudi 1997). Yoshida *et al.* (2002) developed a slope monitoring system with *FBG* borehole inclinometers. Each inclinometer was installed within a casing-tube and had several elements connected to each other with a hinge plate and two sensing tubes. This system had been successfully applied to monitor the deformation of an artificial slope under construction. More recently, Ho *et al.* (2006) developed an *FBG* segmented deflectometer, which can be inserted into the conventional inclinometer casing and measure the relative deflection between the segments of the inclinometer casing.

In this paper, a slope monitoring system developed using the *FBG* technology is presented. The monitoring system consists of an optical sensing interrogator, a multiplexer, and the sensing elements, including the *FBG* strain sensors, *FBG* temperature sensors, and *FBG* in-place inclinometer (*IPI*). After a series of laboratory calibration tests, this system was installed in a roadside slope during the course of slope upgrading works for slope movement monitoring and measurement of strains in slope reinforcements. Monitoring data have been collected during and after the slope stabilization works. Based on the monitoring results, the effects of rainfall on the loading condition of the structural components installed in this slope and slope movements are investigated.

2. *FBG* slope monitoring system

2.1 Sensing principle of FBG

The sensing functioning of *FBG* was firstly discovered on the formation of photo-generated gratings

in germanosilicate optical fibre by Hill *et al.* (1978). Table 1 lists a comparison of features of the conventional sensor and the *FBG* sensor. The Bragg grating is written into a segment of *Ge*- doped single-mode fibre in which a periodic modulation of the core refractive index is formed by exposure to a spatial pattern of ultraviolet (*UV*) light. Fig. 1 illustrates the working principle of an *FBG* sensor. According to Bragg's law, when a broadband source of light has been injected into the fibre, *FBG* reflects a narrow spectral part of light at a certain wavelength (Morey *et al.* 1989).

Table 1 Comparison of features of the conventional sensor and the *FBG* sensor

Content	Conventional sensor	*FBG* sensor
Type	Point sensor	Quasi distributed sensor
Requirement of moisture proof	Yes	No
Data transmission distance	≤100 m	≤10 km
Data collection	Manual in most cases	Automatic
Long-term stability	Poor	Good
Price/performance ratio	Poor	Good

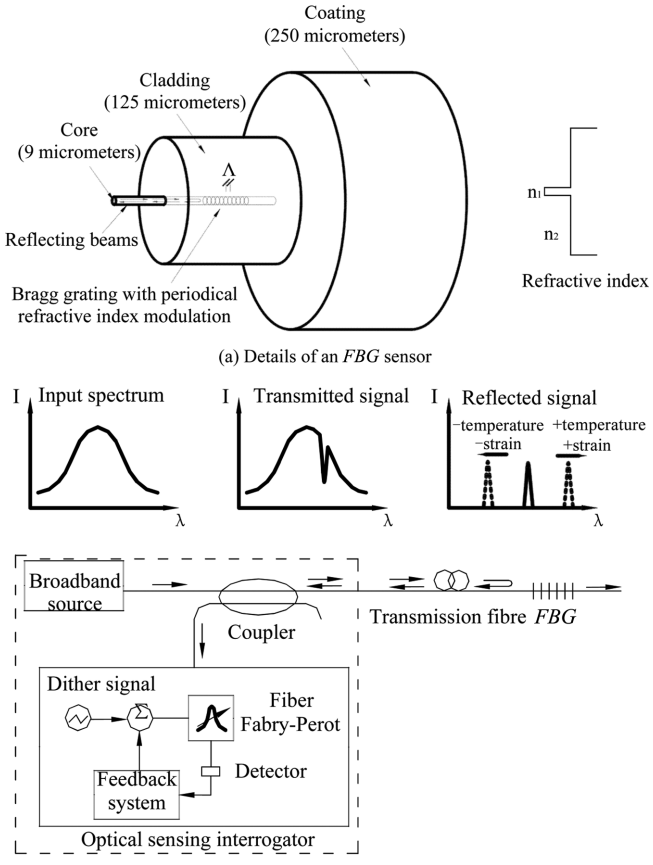

(a) Details of an *FBG* sensor

(b) Strain and temperature sensing of an *FBG* sensor

Fig. 1 Working principle of an *FBG* sensor

$$\lambda_B = 2n\Lambda \tag{1}$$

where λ_B is the Bragg wavelength, typically 1510 to 1590 nm (1 nm = 10^{-9} m); n is the effective core index of refraction; Λ is the period of the index modulation.

Through physical or thermal elongation of the sensor segment and through the change in the refractive index of the fibre due to photo-elastic and thermo-optic effect, the Bragg wavelength will change linearly with strain and temperature. Considering a standard single mode silica fibre, λ_B changes linearly with the applied strain $\Delta\varepsilon$ and temperature ΔT. This relationship is given by (Kersey *et al.* 1997).

$$\frac{\Delta\lambda_B}{\lambda_B} = c_\varepsilon \Delta\varepsilon + c_T \Delta T \tag{2}$$

where λ_B is the original Bragg wavelength under strain free and 0°C condition; $\Delta\lambda_B$ is the variation in Bragg wavelength due to the applied strain and temperature; c_ε and c_T are the calibration coefficients of strain and temperature.

It is worth noting that in order to measure actual strains of a host material, temperature compensation of *FBG* sensors is required. This can be achieved by adding an additional *FBG* sensor to the same temperature field. Once the temperature is measured, the mechanical strain can be corrected as follows

$$\Delta\varepsilon = \frac{1}{c_\varepsilon}\left(\frac{\Delta\lambda_B}{\lambda_B} - c_T \Delta T\right) \tag{3}$$

2.2 Functions of the slope monitoring system

Based on *FBG* sensing technology, a slope monitoring system is established, which is depicted in Fig. 2. The following functions are included in this system.

(1) The measurement of slope movements and strains/stresses within the structural components.

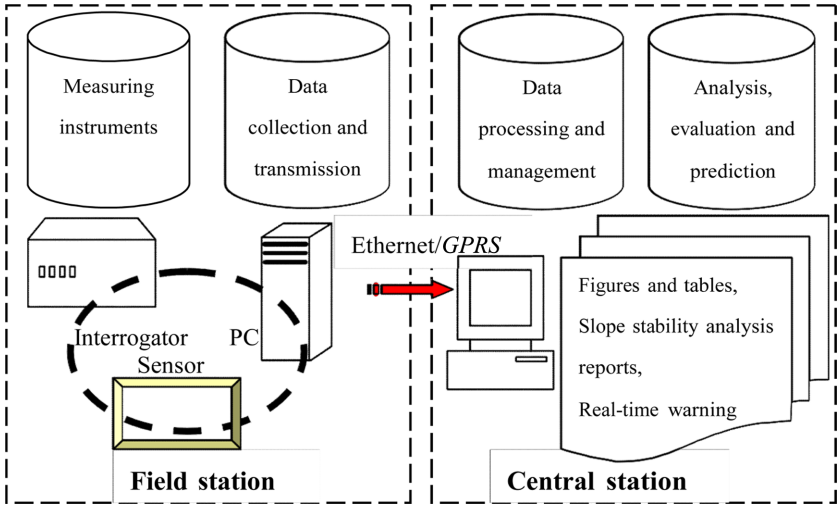

Fig. 2 Schematic illustration of the *FBG* slope monitoring system

The utilization of newly developed *FBG* sensors allows the measurement of a variety of parameters. The *FBG* sensors can be connected in series to form a quasi-distributed sensing array.

(2) The collection and transmission of monitoring results. An optical sensing interrogator is employed to measure the *FBG* wavelength readings. The Ethenet and General packet radio service (GPRS) can be used in the field for data transmission.

(3) The processing and management of monitoring results. A computer is used to record and store all the monitoring data in real-time.

(4) Slope stability analysis and performance evaluation. Based on the monitoring data, the location of the potential slip surface of the slope under investigation can be estimated and slope stability analysis can be conducted.

2.3 Development and calibration of FBG sensors

2.3.1 FBG strain sensor

A series of laboratory calibration tests were conducted to examine the reliability of *FBG* strain sensors. First, the *FBG* strain sensors and electrical strain gauges were adhered on six steel bars with a

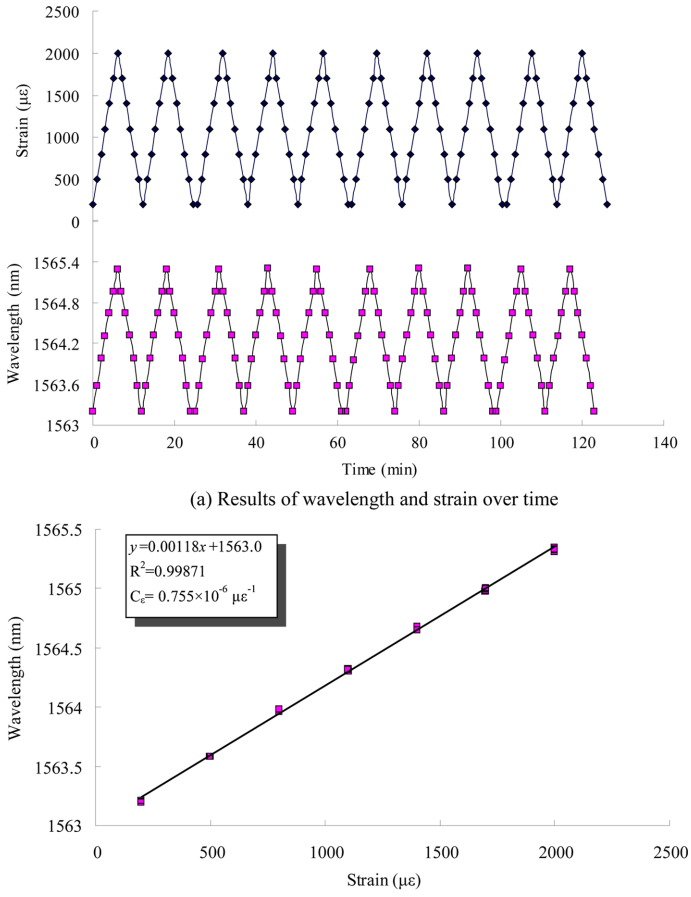

(a) Results of wavelength and strain over time

(b) Relationship between wavelength and applied strain

Fig. 3 Typical calibration results of the *FBG* surface adhered strain sensor

diameter of 10, 25, and 32 mm, respectively. Tensile strains were then applied on the steel bars in stages using a universal testing machine and ten loading and unloading cycles were conducted. Typical calibration test results are shown in Fig. 3. The relationship between the Bragg wavelength of every *FBG* sensor and the applied tensile strain is fairly linear with R^2 of over 0.99 and no hysteretic or fatigue effects were observed during testing. This demonstrates the effectiveness of *FBG* used as a strain sensor. From the results, an average strain calibration coefficient c_ε of 0.755×10^{-6} $\mu\varepsilon^{-1}$ is obtained. As the accuracy of the *FBG* interrogator system is 1 pm (10^{-12} m), the strain accuracy is estimated to be 0.83 $\mu\varepsilon$.

2.3.2 FBG temperature sensor

For temperature compensation of strain, a tube packaged *FBG* temperature sensor is developed. The temperature sensor consists of a loose *FBG* sensor encapsulated in a 5 mm diameter steel tube. In field applications, this sensor will be mechanically uncoupled from but in thermal contact with the host material.

For calibration purpose, the *FBG* temperature sensors were immersed into a temperature controlled water bath, together with a type-*K* thermocouple. A digital thermometer was used to measure the temperature variation during testing. Typical calibration results presented in Fig. 4 show that there is a linear relationship between the Bragg wavelength and the applied temperature. The average temperature calibration coefficient is calculated to be $6.38\times10^{-6}{}^{o}C^{-1}$ and thus the temperature accuracy of the *FBG* sensor is 0.10^{o}C.

2.3.3 FBG in-place inclinometer

For internal displacement measurement of geotechnical structures such as foundations, dams or slopes, the inclinometer plays a dominant role. Based on *FBG* sensing technology, an innovative *FBG* in-place inclinometer has been developed by the authors in The Hong Kong Polytechnic University. In this inclinometer, a conventional polyvinyl chloride (PVC) inclinometer casing with an outer diameter of 60 mm and an internal diameter of 50 mm is designed to be instrumented with quasi-distributed *FBG* sensors. Four optical fibres containing a series of *FBG* strain sensors at regular intervals are adhered in the orthogonal grooves of the casing and covered by epoxy resin.

According to Euler-Bernoulli beam theory, the strain distributions on the casing surface are associated with the distributions of normal axial force and bending moment along the neutral line. The strains can be converted into the deflections of the casing by

$$\begin{cases} u = \dfrac{1}{R}\iint \varepsilon^{Tx}(z)dzdz \\ v = \dfrac{1}{R}\iint \varepsilon^{Ty}(z)dzdz \end{cases} \tag{4}$$

where u and v are deflections of the casing in the x and y directions, respectively; $\varepsilon^{Tx}(z)$ and $\varepsilon^{Ty}(z)$ are the strains due to transverse loading in the x and y directions, respectively; R is the outer diameter of the casing.

Taking ε_a, ε_b, ε_c and ε_d as the strains measured by the four surface adhered *FBG* sensors on a specific section of this casing, respectively, the axial strains associated with bending of the casing induced by transverse loading can be calculated as $\varepsilon^{Tx} = \frac{1}{2}(\varepsilon_a - \varepsilon_c)$ and $\varepsilon^{Ty} = \frac{1}{2}(\varepsilon_b - \varepsilon_d)$.

As the quasi-distributed *FBG* sensors measure strains at discrete points, linear interpolation of strain distributions is selected to calculate the distributions of deflection of the casing for its simplicity.

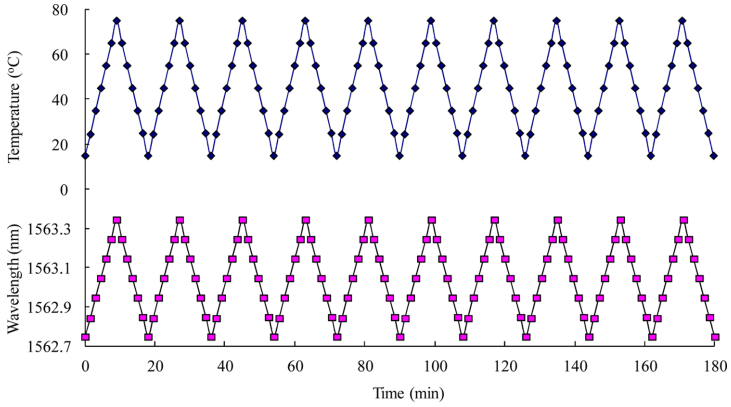

(a) Results of wavelength and temperature over time

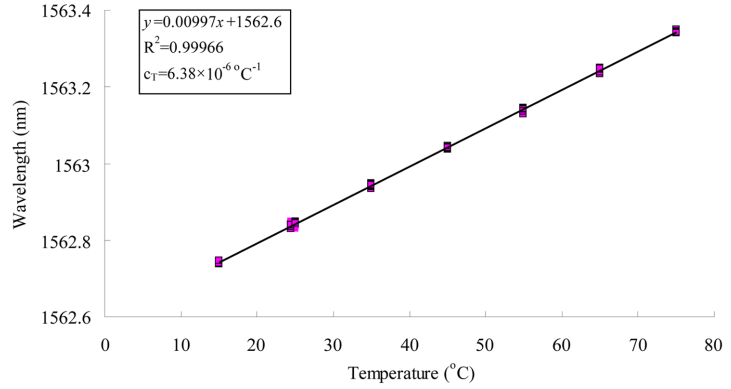

(b) Relationship between wavelength and applied temperature

Fig. 4 Typical calibration results of the tube packaged *FBG* temperature sensor

However, this will bring some errors in deflection calculation. To compute deflections on the basis of strain distributions, it is necessary to specify boundary conditions of the *FBG* inplace inclinometer. If the inclinometer tip is buried in a considerably deep position (such as below the bed rock), then a fixed end can be assumed and the relationships of $u_{z=0} = v_{z=0} = 0$ and $\left(\frac{du}{dz}\right)_{z=0} = \left(\frac{dv}{dz}\right)_{z=0} = 0$ can be applied.

A series of laboratory calibration tests were conducted on the *FBG* in-place inclinometer. As shown in Fig. 5, the inclinometer casing was simply supported and the deflections were applied by weight sets in stages during testing. The calibration results show that the displacements measured by the *FBG* in-place inclinometer fit well with those measured by dial gauges. The test results validate the performance and accuracy of the *FBG* in-place inclinometer in capturing deflections along the casing.

3. Field instrumentation of a roadside slope

3.1 Project background

A trial of this *FBG* slope monitoring system has been successfully conducted on a roadside slope

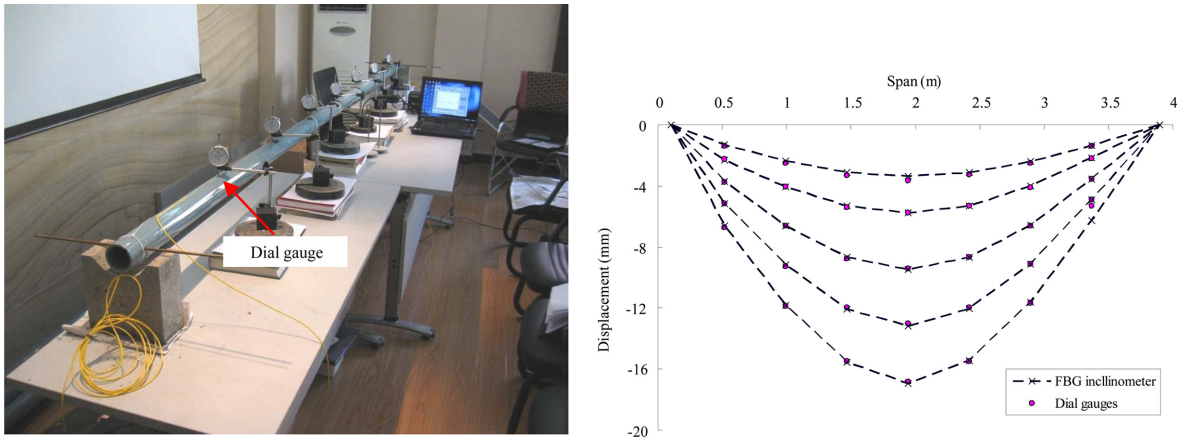

(a) Calibration test set-up (b) Typical calibration results

Fig. 5 Laboratory calibration of the *FBG* in-place inclinometer

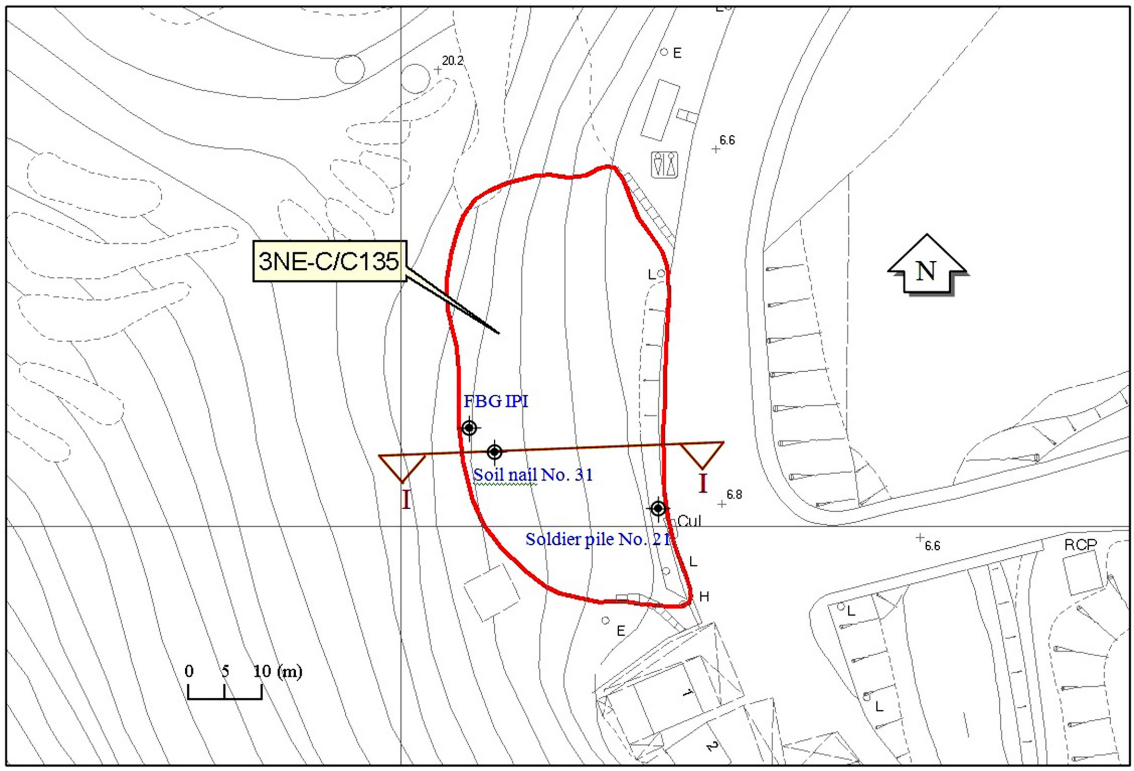

Fig. 6 Location of the instrumented slope site

in Hong Kong, when slope upgrading works were being implemented. The slope site under investigation is located at Luk Keng Road, Sheung Shui, New Territories, Hong Kong (Slope Registration No. 3NE-C/C135) (see Fig. 6). A major portion of this roadside slope is owned by the government and it has a height of 10 m, a length of 51 m, and a slope angle of 35°.

The geological conditions of the slope site are depicted in Fig. 7. From top to bottom, the slope

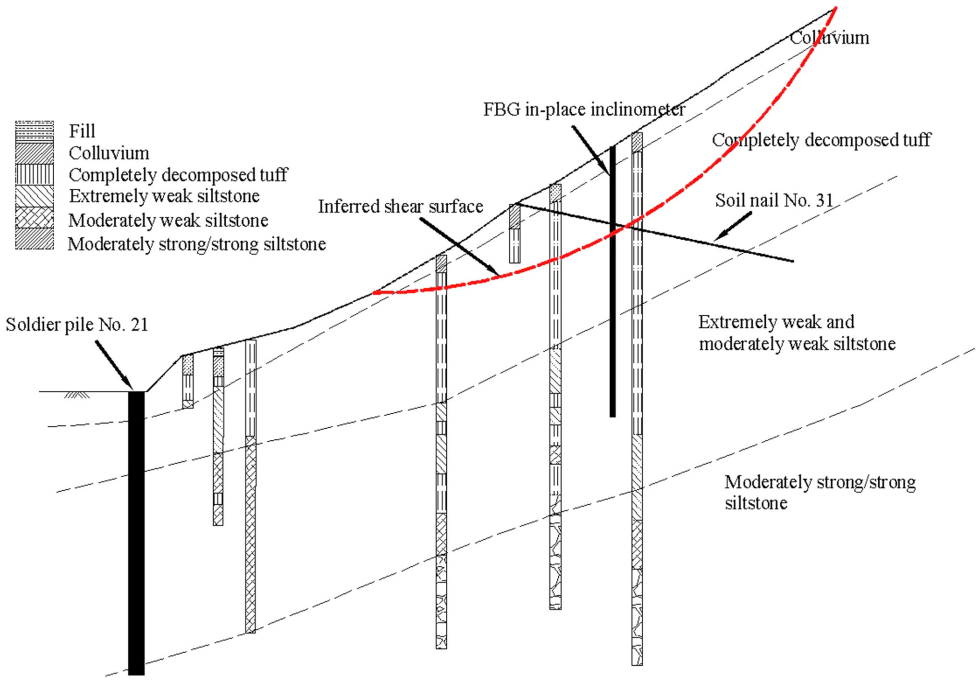

Fig. 7 Geological conditions of the slope site (Section I-I)

consists of layers of colluvium, completely decomposed tuff, extremely weak to moderately weak siltstone, and the underlying rock layer. The layer of weak siltstone is very permeable and is conducive in directing concentrated subsurface water flow from the hillside above towards the slope toe. The groundwater regime in this area is also affected by the tidal effects of Sha Tau Kok Hoi, which tends to control deeper groundwater movements. During and soon after heavy rainfall, groundwater from surface infiltration in the upper catchment is channelled towards the toe of the slope, causing an abrupt rise in groundwater level. Previous monitoring data reveal that the slope is subjected to rapid rise and upward flow of groundwater near the slope toe soon after heavy rainfall. Inclinometers installed in the slope also indicated lateral ground movements back and forth, and localized deformation and distress were observed in the vicinity of the slope toe. The potential instability of the slope poses a threat not only to the normal operation of the road that runs parallel to the slope toe, but also to the safety of nearby residents.

Under the Landslip Preventive Measures Programme (dovetailed by the long-term Landslip Prevention and Mitigation Programme since 2010) managed by the Geotechnical Engineering Office (*GEO*), Civil Engineering and Development Department (*CEDD*) of the Government of the Hong Kong Special Administrative Region (*HKSAR*), the slope was selected for stability study and implementation of upgrading works. Slope stabilization measures including soil nails, toe-support soldier piles, and drainage facilities were designed and the construction works were supervised by Ove Arup & Partners Hong Kong Limited, a geotechnical consultant to the *GEO*.

To facilitate post-construction review of the slope performance and the effectiveness of the stabilization measures, a conventional geotechnical monitoring system was installed as part of the slope works. The optical fibre monitoring system based on *FBG* technology was also initiated by Ove Arup & Partners Hong Kong Limited and installed in this slope by the authors in The Hong

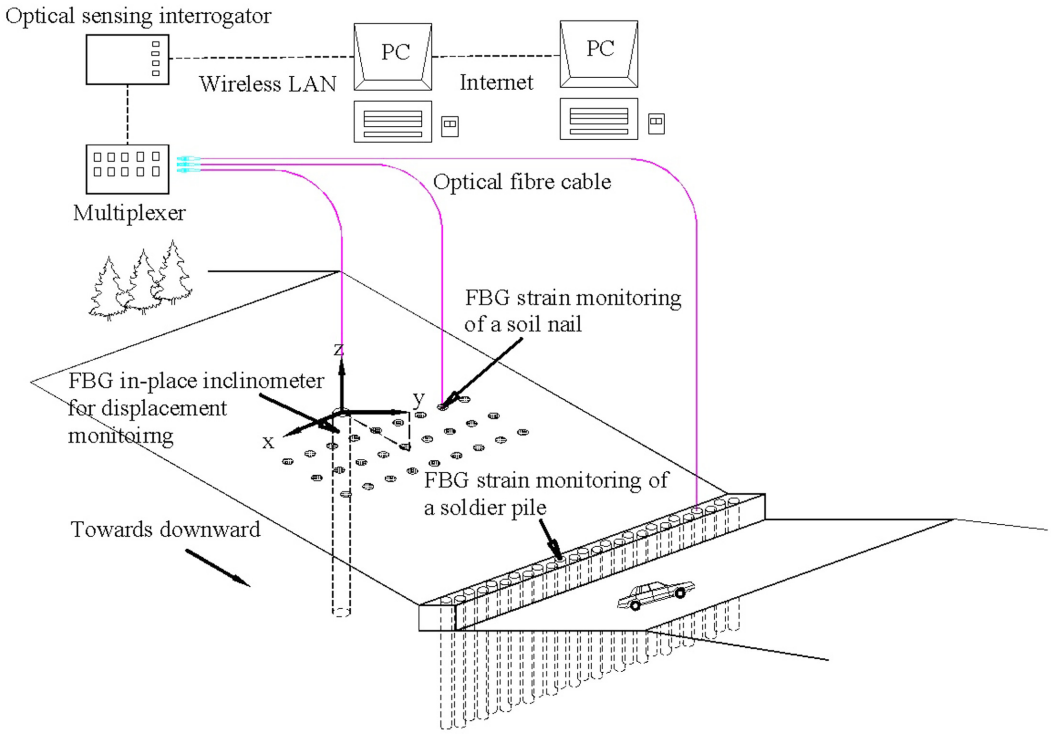

Fig. 8 Illustration of the instrumentation of the roadside slope

Kong Polytechnic University as a trial for assessing the reliability of the system. The data collected by the integrated *FBG* sensing and monitoring system were used for evaluating the performance of the stabilization measures. The key measurements are (a) tensile forces in a soil nail; (b) loading condition of a soldier pile; and (c) slope movements. The general arrangement of the optical fibre monitoring system at this slope site is illustrated in Fig. 8. With the multiplexing operation in this *FBG* sensor system, only one optical sensing interrogator with a multiplexer is needed for site measurements.

3.2 Installation of FBG sensors on a soil nail and a soldier pile

As part of the slope stabilization works, a total of 37 soil nails (4 rows) were installed. The nail length varies from 12 to 14 m, with a uniform spacing of 2 m between two adjacent nails. The design load of each nail is in the range of 40 to 54 kN. These soil nails were installed in 150 mm diameter drillholes. During soil nail installation, the galvanized steel bars of 25 mm in diameter are inserted into the drillhole and grouted with cement grout.

In general, soil nails are used to resist the ground movement above the potential sliding surfaces in the slope by the mobilization of tensile forces. In order to capture the development of axial forces in the soil nails, a 14 m-long soil nail (Soil nail No. 31) was instrumented with 10 surface glued *FBG* strain sensors along the nail length, where 10 corresponding *FBG* tube packaged temperature sensors were installed for temperature compensation (see Figs. 9 and 10). The axial force along the soil nail is estimated as follows

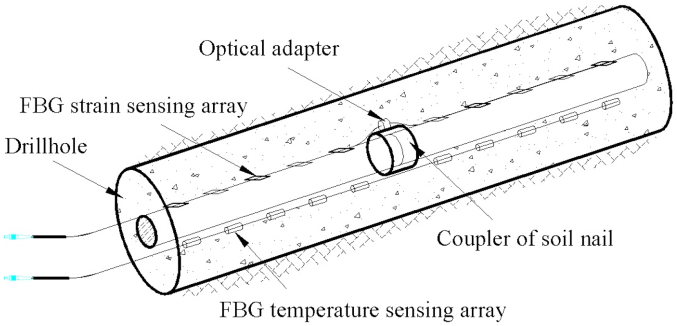

Fig. 9 *FBG* strain sensors installed on the soil nail

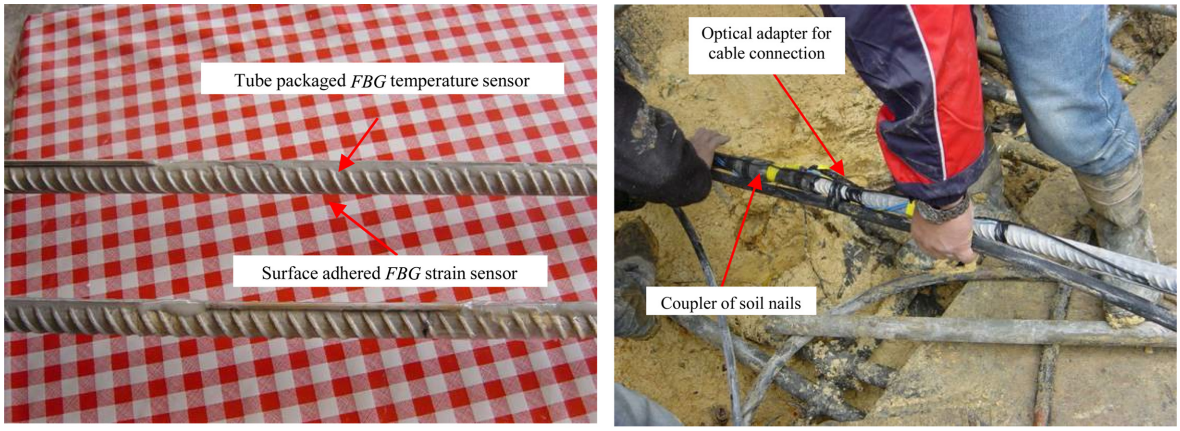

(a) Details of the soil nail instrumented with *FBG* strain and temperature sensors prior to installation

(b) Connection of optical fibre cables at the coupling part during soil nail installation

Fig. 10 Installation of the instrumented soil nail on site

$$T_i = (A_S E_S + A_C E_C)\varepsilon_i \tag{5}$$

where ε_i is the strain measured by the ith *FBG* strain sensor corrected by the ith *FBG* temperature sensor; A_S, A_C are the cross sectional areas of the steel bar and the cement grout, respectively; E_S, E_C are the Young's moduli of the steel bar and the cement grout, respectively. In view of possible cracks that might develop in the cement grout, a reduced modulus for E_c was adopted in the estimation of the tensile force that developed in the soil nail.

Two rows of soldier piles were also installed at the slope toe to provide lateral support to the slope mass. The 16 m-long soldier piles with a diameter of 550 mm were installed at 1.8 m intervals. They pass through the potential sliding surfaces and are embedded in the competent rock strata to provide anchorage against the sliding forces. For each soldier pile, a 305×305×198 kg/m *H*-shaped steel column was inserted in a borehole which was filled with cement grout. For the soldier piles, the main purpose of optical fibre monitoring is to verify their effectiveness to stabilize the slope and provide data for performance review. One of the piles (Soldier pile No. 21) was selected for monitoring using 18 *FBG* strain sensors and 9 temperature sensors, as shown in Figs. 11 and 12. The *FBG* sensors were glued onto the two flanges of the steel column and a series of *PVC* trunkings were used to protect the optical fibre cables from potential damage. Using the monitoring

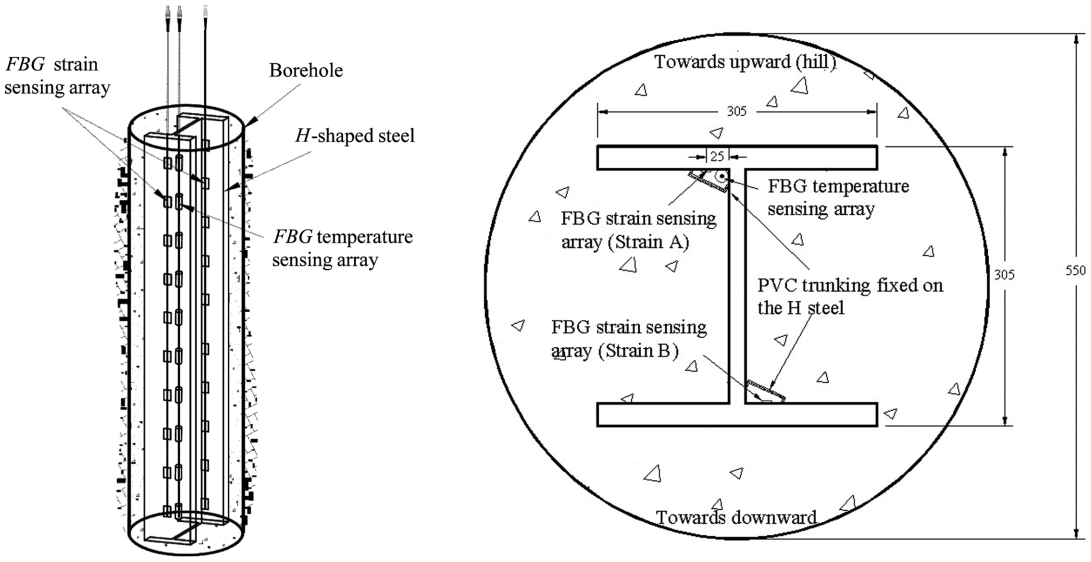

(a) Side view (b) Sectional view (unit: mm)

Fig. 11 *FBG* strain and temperature sensors installed on the soldier pile

(a) Installation of *FBG* strain and temperature sensors (b) Embedding and grouting the *H*-shaped steel pile

Fig. 12 Photographs of the instrumented soldier piles during installation

data, information on the bending moments and shear forces in the pile can be deduced and the variations of the net lateral load from the groundmass above can be estimated.

3.3 Installation of a FBG in-place inclinometer

As indicated by previous monitoring data and geotechnical assessment, there may be a number of sliding surfaces or shear zones within the slope. However, it was uncertain if the locations of these sliding surfaces/shear zones might change with time. In order to assess the magnitude and direction of slope movements and to provide data for assessment of the performance of the slope stabilization measures installed, an *FBG* in-place inclinometer was installed in a 120 mm diameter, 15 m deep

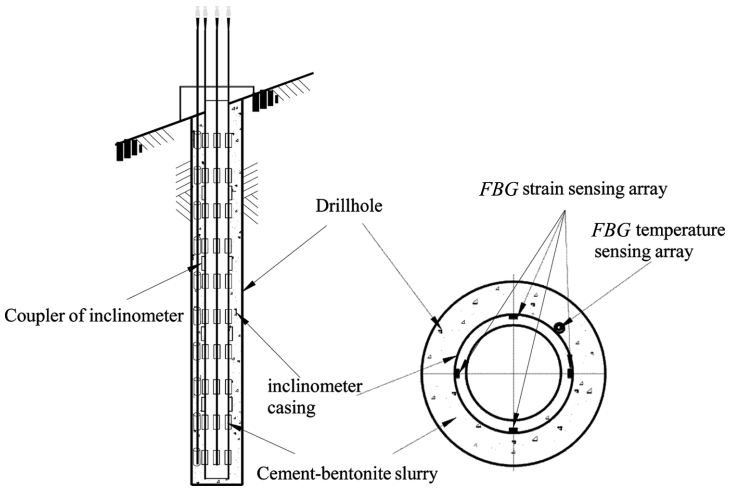

Fig. 13 *FBG* in-place inclinometer installed in the slope site

(a) Details of the *FBG* inclinometers prior to installation (b) Coupling and installation of the *FBG* inclinometer

Fig. 14 Photographs of the *FBG* in-place inclinometer during installation

drillhole in the slope (see Fig. 13). On the in-place inclinometer, four optical fibres each containing ten *FBG* strain sensors at 1.5 m intervals were adhered in the orthogonal grooves in the inclinometer casing and were protected with an epoxy resin cover. An additional optical fibre with ten *FBG* temperature sensors was attached to the casing for temperature compensation of the strain measurements. The *FBG* inclinometer casing was assembled in the field section by section and grouted in the drillhole using a cement bentonite grout (see Fig. 14). The monitoring results of the *FBG* inclinometer can be used to calculate the lateral ground displacements in the x (approximately across the slope) and y (approximately down the slope) directions and to estimate the locations with potential movement.

It's worth noting that the bare *FBG* sensors are fragile and can hardly survive adverse conditions in a construction site. To provide protection to the *FBG* sensors, a sensor and cable protection system including plastic and metal tubes, optical fibre splice closures and distribution boxes were

adopted. As the *FBG* sensors were connected in series, a configuration of optical fibre loop was utilized to reduce the risk of data loss resulting from sensor malfunctions or breaking of fibre. Notwithstanding this, several armoured cables on the soldier pile were severely damaged during construction and only four *FBG* signals were detected eventually.

4. Monitoring results and analysis

Monitoring data was retrieved on site using a multiplexer and an optical sensing interrogator. The data was transmitted back to the laboratory via wireless data connections. Selected monitoring data are presented in Figs. 15 to 18.

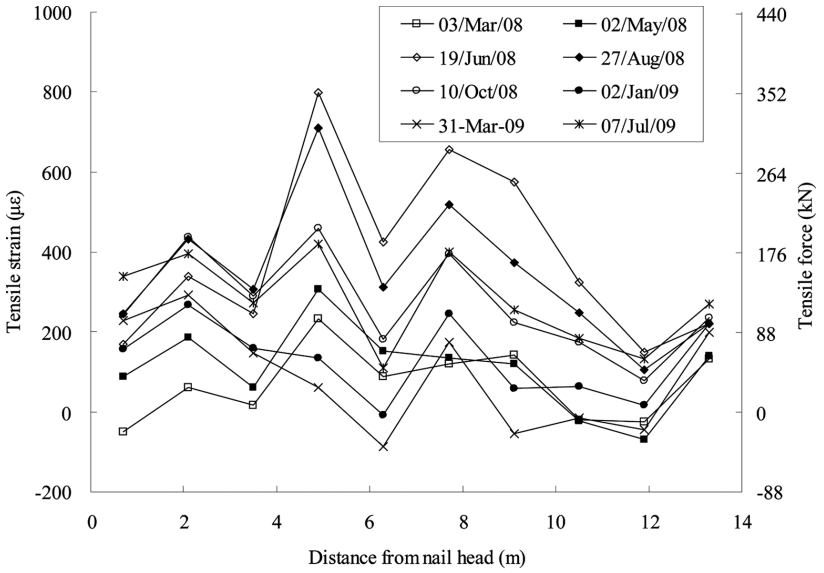

(a) Measured strains on the soil nail

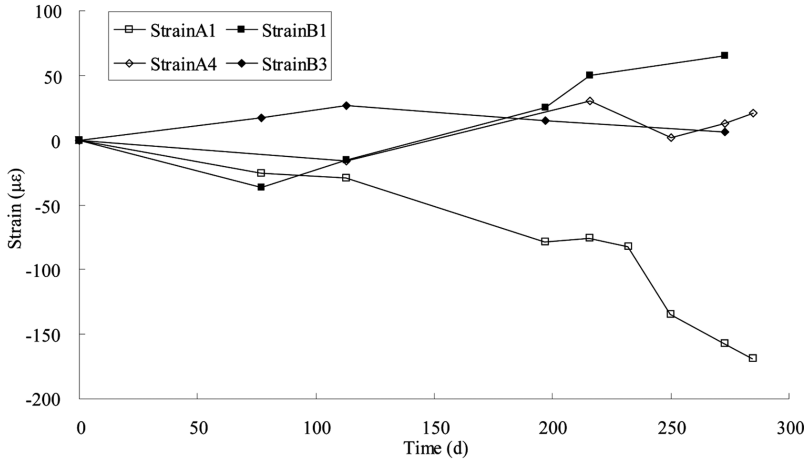

(b) Measured strains on the soldier pile

Fig. 15 Strains on the soil nails and soldier pile measured by *FBG* sensors

4.1 Strain variations in the soil nail and the soldier pile

Fig. 15(a) shows the monitoring results of tensile strain and the deduced axial force on the soil nail. The soil nail was subjected to tensile stresses in general and the strains developed gradually on the soil nail. A maximum strain of over 800 $\mu\varepsilon$ was observed at 5 m from the nail head on 19 June 2008 after a period of heavy rainfall and prior to the completion of the slope upgrading works. The readings of the vibration wire strain gauges that were surface mounted on Soil nail No. 32, the neighbouring soil nail, were recorded on 21 June 2008. The strain gauges measured a maximum strain of 802 $\mu\varepsilon$, which occurred near the mid-span of the soil nail. This indicates that the *FBG* strain readings should be reliable. After June 2008, the strains of all the *FBG* strain sensors started to reduce as time elapsed. The location of maximum strain moved to the slope surface. When rainy season came again, the maximum strain increased sharply. This indicates the loading condition of the soil nails is adaptive with the slope condition. There is an inherent interaction between the soil nails and the slope mass.

For the soldier pile, the *FBG* strain sensors Strain A1 and B1 near the pile head showed significant variations in magnitude over time, as shown in Fig. 15(b). Changes in strain levels in the pile can be related to changes in the forces exerted by the slope mass above the pile as well as the pile's interaction with the reinforced concrete toe wall connected to the pile head. For *FBG* strain sensors Strain A4 and B3, which are at 5.5 and 4 m depths below the ground surface, the strains remain at a relatively small level, indicating some spare capacity in the steel column. As there was no conventional sensor on the soldier pile, the comparison of monitoring results cannot be conducted.

To study the effect of rainfall on performance of soil nails and soldier piles, the strain of the soil nail at 5 m from the nail head and the strain of the soldier pile at 1 m depth were selected. The tendency of strain curves in Fig. 16 indicates that the variation in tensile force of the soil nail is generally consistent with monthly rainfall. The rise of groundwater level during the rainy seasons led to reduction of shear strength and increase in loading from the slope mass on the nail. For the soldier pile, the *FBG* strain sensors near the pile head showed some variations in strain magnitude over time but there is not a consistent relationship between strain and monthly rainfall.

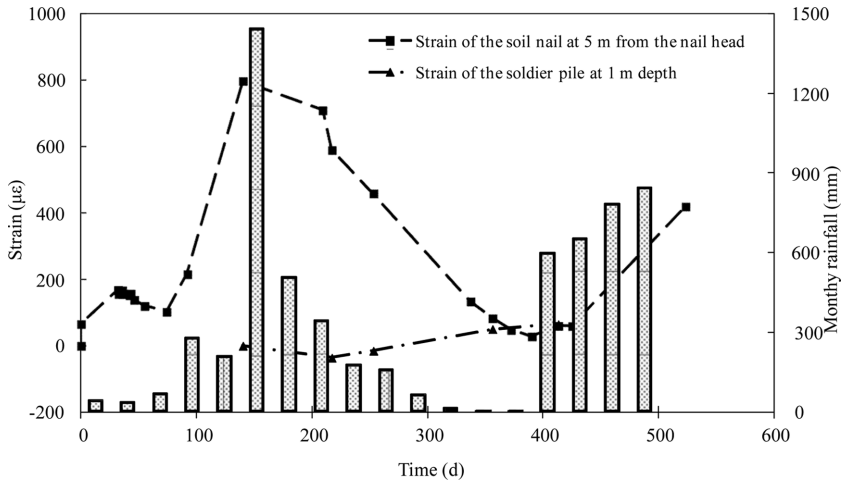

Fig. 16 Monitoring results of the strains in the soil nail and the soldier pile by *FBG* sensors and rainfall record

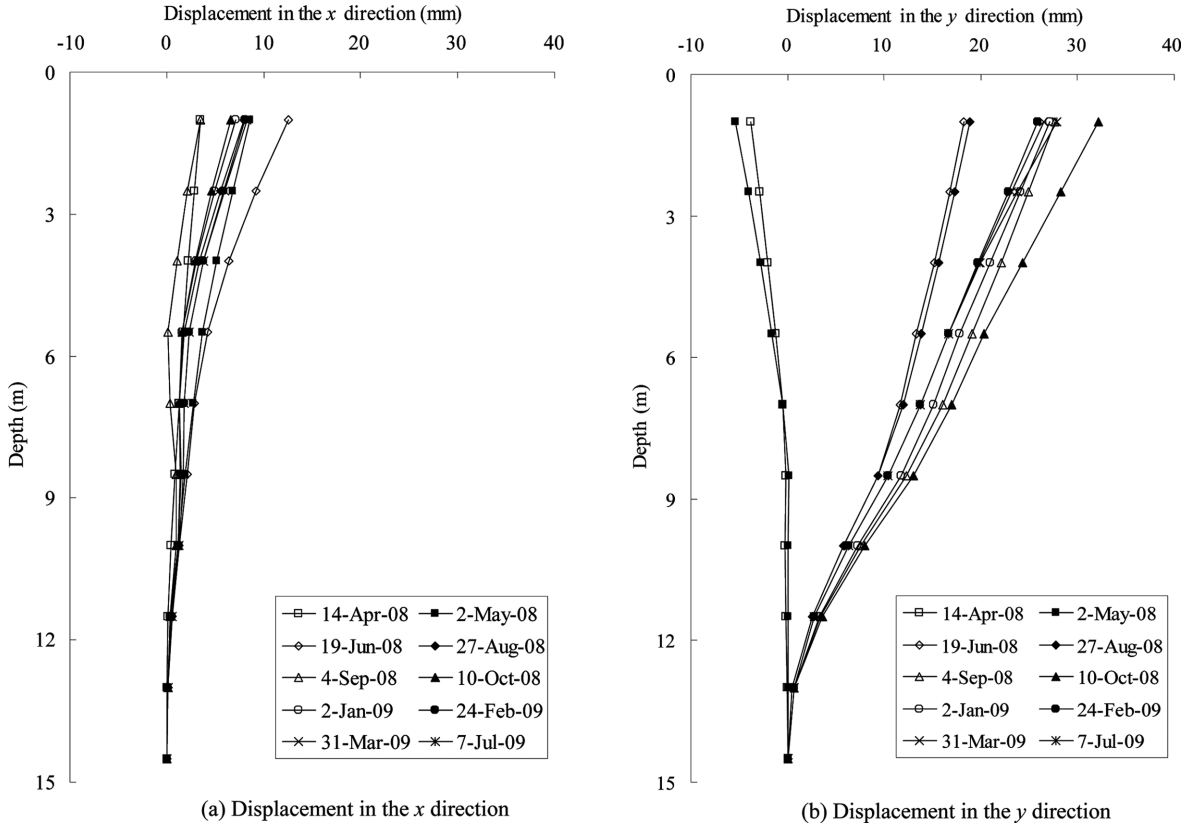

Fig. 17 Monitoring results of the slope movements by the *FBG* in-place inclinometer

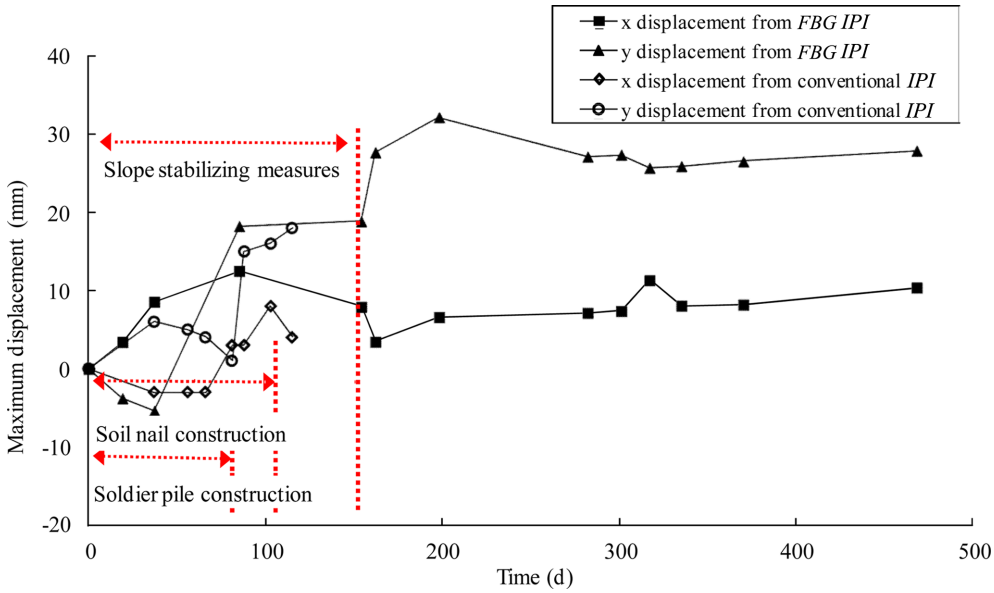

Fig. 18 Monitoring results of maximum slope movements in the *x* and *y* directions with respect to time

4.2 Slope movements

From the monitoring data in Fig. 17, the slope movements accumulated gradually. The slope mass also moved laterally (in the x direction), apart from moving downslope in the y direction. This could have been the result of influences from the orientation of weak zones within the slope mass. As shown in Fig. 18, the magnitudes of maximum displacement measured by the *FBG* in-place inclinometer and the conventional in-place inclinometer installed nearby are close. After the completion of the slope improvement measures, no further notable movement of the slope is detected.

5. Conclusions

The provision of geotechnical field instrumentation for slope monitoring is a very challenging task for the geotechnical profession, given the current status of available technologies. This is particularly difficult if the slope concerned is far away from urban areas, as requirements for automation, integration and remote data transmission in slope instrumentation are of great importance. The experience gained from this work leads to the following conclusions:

(1) The slope monitoring project introduced in this paper provides a good example for showing the feasibility of optical fibre sensing technology for use in long-term field monitoring of slopes. Apart from other field measurement technologies, *FBG* is of high resolution and high resistance to *EMI*. Coupled with multiplexible capacity, the technology is suitable for use in slope monitoring.

(2) The slope monitoring results reaffirm our understanding that the rainfall infiltration and rise in groundwater pressures will lead to mobilization of tensile forces in soil nails. The slope movements developed in a three-dimensional pattern may have been affected by the orientation of weak zones within the slope mass.

From an application point of view, optical fibre sensing technology in the area of slope instrumentation is still being developed, and has not been widely recognized by the practitioners. Past experiences, including the experience gained by the authors in this project, indicate that close collaboration and teamwork of experienced geotechnical engineers, optoelectronic engineers and technical staff in field installation is a prerequisite for establishing a reliable optical fibre slope monitoring system for geotechnical structures. In building an effective, reliable and economical slope monitoring system, the optical fibre sensing technology has shown very good potential for further development and applications.

Acknowledgements

The financial supports provided by The Hong Kong Polytechnic University (Grant No. G-YE54, 1-BB7U and G-YG60) for the development of *FBG* sensors for slope monitoring are gratefully acknowledged. This research is partially supported by the National Basic Research Program of China (973 Program) (Grant No. 2011CB710605) and the National Key Technology R&D Program of China (2012BAK10B05). The support-in-kind from both Ove Arup & Partners Hong Kong Limited and the *GEO*, *CEDD* in facilitating the field instrumentation and monitoring of the subject slope in the slope upgrading works project is acknowledged. This paper is published with the permission of the Head of the *GEO* and the Director of *CEDD* of the HKSAR Government.

References

Ding, X.L., Huang, D.F., Yin, J.H., Chen, Y.Q., Lau, C.K., Yang, Y.W., Sun, Y.R., Chen, W. and He, X.F. (2003), "Development and field testing of a multi-antenna GPS system for deformation monitoring", *Wuhan Univ. J. Nat. Sci*., **8**(2), 671-676.

Dunnicliff, J. (1993), *Geotechnical instrumentation for monitoring field performance*, John Wiley & Sons Inc, New York.

Fredlund, D.G. and Rahardjo, H. (1993), *Soil mechanics for unsaturated soils*, John Wiley & Sons Inc, New York.

Kersey, A.D., Davis, M.A., Patrick, H.J., LeBlanc, M., Koo, K.P. Askins, C.G., Putnam, M.A. and Friebele, E.J. (1997), "Fiber grating sensors", *J. Lightwave Technol*., **15**(8), 1442-1463.

Gasmo, J., Hritzuk, K.J., Rahardjo, H. and Leong, E.C. (1999), "Instrumentation of an unsaturated residual soil slope", *Geotech. Test. J*., **22**(2), 128-137.

Hill, K.O., Fujii, Y., Johnson, D.C. and Kawasaki, B.S. (1978), "Photosensitivity in optical fiber waveguides: application to reflection filter fabrication", *Appl. Phys. Lett*., **32**(10), 647-649.

Ho, Y.T., Huang, A.B. and Lee, J.T. (2006), "Development of a fibre Bragg grating sensored ground movement monitoring system", *Meas. Sci. Technol*., **17**(7), 1733-1740.

Inaudi, D. (1997), *Fiber optic sensor network for the monitoring of civil engineering structures*, PhD Thesis, EPFL, Lausanne, Switzerland.

Li, A.G., Yue, Z.Q., Tham, L.G., Lee, C.F. and Law, K.T. (2005), "Field-monitored variations of soil moisture and matric suction in a saprolite slope", *Can. Geotech. J*., **42**(1), 13-26.

Lin, C.P. and Tang, S.H. (2005). "Development and calibration of a *TDR* extensometer for geotechnical monitoring", *Geotech. Test. J*., **28**(5), 1-8.

Millis, S.W., Ho, A.N.L., Chan, E.K.K., Lau, K.W.K. and Sun, H.W. (2008), "Instrumentation and real time monitoring of slope movement in Hong Kong", *Proceedings of the12th International Conference of International Association for Computer Methods and Advances in Geomechanics*, Goa, India.

Morey, W.W., Meltz, G. and Glenn, W.H. (1989), "Fiber optic bragg grating sensors", *Proceedings of the SPIE*.

Ng, C.W.W., Zhan, L.T., Bao, C.G., Fredlund, D.G. and Gong, B.W. (2003), "Performance of an unsaturated expansive soil slope subjected to artificial rainfall infiltration", *Geotechnique*, **53**(2), 143-157.

Peyret, M., Djamour, Y., Rizza, M., Ritz, J.F., Hurtrez, J.E., Goudarzi, M.A., Nankali, H., Chéry, J., Le Dortz, K. and Uri, F. (2008), "Monitoring of the large slow Kahrod landslide in Alborz mountain range (Iran) by GPS and SAR interferometry", *Eng. Geol*., **100**(3-4), 131-141.

Wong, H.N., Ho, K.K.S. and Sun, H.W. (2006), "The role of slope instrumentation in landslide risk management-Hong Kong experience", *Proceedings of the Conference on Landslide*, Sinkhole, Ipoh, Malaysia.

Yin, J.H., Ding, X.L., Yang, Y.W., Lau, C.K., Huang, D.F. and Chen, Y.Q. (2004), "Integration of conventional instruments and global positioning system for automatic monitoring of slopes", *Chin. J. Rock Mech. Eng*., **23**(3), 357-364. (in Chinese)

Yoshida, Y., Kashiwai, Y., Murakami, E., Ishida, S. and Hashiguchi, N. (2002), "Development of the monitoring system for slope deformations with fiber Bragg grating arrays", *Proceedings of the SPIE*.

Zhang, T.L.T., Ng, C.W.W. and Fredlund, D.G. (2006), "Instrumentation of an unsaturated expansive soil slope", *Geotech. Test. J*., **30**(2), 1-11.

JK